crystals

MDPI

Article

Design and Synthesis of Multicomponent Re(IV)-Containing Magnetic Materials Toward Optoelectronics

Andrzej Kochel [1,*], Małgorzata Hołyńska [2,*], Natalia Mikłuszka [1] and Zoe Fard [3]

[1] Faculty of Chemistry, University of Wrocław, ul. F. Joliot Curie 14, 50 383 Wrocław, Poland; natalia.mikluszka@phd.uwr.edu.pl
[2] European Space Research and Technology Centre, Keplerlaan 1, 2200 AZ Noordwijk, The Netherlands
[3] Petro-Canada Lubricants, 385 Southdown Rd, Mississauga, ON L5J 2Y3, Canada
* Correspondence: andrzej.kochel@uwr.edu.pl (A.K.); malgorzata.holynska@esa.int (M.H.)

Abstract

The reaction of $(NH_4)_2ReCl_6$ with cyclohexylamine yielded the rhenium(IV) salt in the form of dihydrate $(C_6\ H_{14}\ N)_{10}\ (ReCl_6)_3{\cdot}4Cl{\cdot}2(H_2O)$, where $C_6H_{14}N$ is protonated cyclohexylamine. Its uncommon stoichiometry distinguishes it from typical hexachloridorhenates(IV) compounds used as model systems and dopants in optoelectronic materials. Magnetic studies showed antiferromagnetic properties at low temperatures. Crystal structure analysis revealed a three-dimensional hydrogen bonding network formed by cyclohexylammonium cations and water molecules.

Keywords: crystal structure; magnetic properties; 3D hydrogen bonding system

1. Introduction

Rhenium(IV) compounds have attracted increasing attention due to their unique electronic, optical, and magnetic properties. In particular, transition-metal dichalcogenides (TMDs), such as ReS_2, exhibit unique anisotropic optical behaviors, making them promising materials for advanced space applications. These materials are emerging as key enablers of optoelectronic systems for space exploration and satellite technologies. For instance, ReS_2 nanosheets act as highly efficient saturable absorbers, enabling the development of ultrafast (femtosecond) pulsed lasers for space-based optical communication networks and LiDAR remote sensing [1].

Moreover, the inherent stability of two-dimensional ReS_2, combined with its strong absorption coefficients and robust bandgap properties, makes it an ideal candidate for radiation-hardened photodetectors. Such devices are essential for highly sensitive optical sensors capable of operating under the harsh cosmic radiation conditions encountered in Low Earth Orbit (LEO) and deep-space missions [1–3]. Consequently, understanding the behavior of rhenium(IV) compounds is important for the development of next-generation resilient optoelectronic systems tailored to the demands of space applications. Hexachloridorhenates(IV) are considered model compounds for investigating the general behavior of rhenium(IV) systems, due to their stability and interesting magnetic properties [4–10]. They are used as precursors and hybrid material components. In addition, such anions serve as dopants or functional anionic complexes in lead-free vacancy-ordered double perovskites and metal halide lattices, where they play important roles in near-infrared (NIR) light sources, optical temperature sensors, and non-destructive inspection devices [11].

Check for updates

Academic Editors: Ana M. Garcia-Deibe and Jesús Sanmartín-Matalobos

Received: 3 October 2026
Revised: 13 November 2026
Accepted: 16 November 2026
Published: 20 November 2026

Copyright: © 2026 by the authors. Licensee MDPI, Basel, Switzerland. This article is an open access article distributed under the terms and conditions of the Creative Commons Attribution (CC BY) license.

In this report, we present a rare case of a multicomponent crystal containing hexachloridorhenate(IV) anions with solvent molecules adding a hydrogen bonding network and influencing the overall magnetic properties.

2. Materials and Methods

2.1. Synthesis and Crystallization

Preparation of $(C_6\ H_{14}\ N)_{10}\ (ReCl_6)_3{\cdot}4Cl{\cdot}2(H_2O)$.

All reagents were obtained from Merck KGaA (Darmstadt, Germany). $(NH_4)_2ReCl_6$ was obtained by the reaction of NH_4ReO_4 with H_3PO_2 in a 7 M solution of HCl [12]. $(NH_4)_2ReCl_6$ (0.17 g) was dissolved in double-distilled water (80 mL) with concentrated (36%) HCl (1.5 mL) and the mixture was heated under reflux at 340 K. After 20 min, cyclohexylamine (0.27 g) was added, and the mixture was heated for an additional 8 h. After cooling, the yellow–green precipitate was filtered off and washed with ethanol 96% (Scheme 1). Crystals for X-ray study were obtained by slow evaporation of an aqueous solution of precipitate with addition of 1 mL of HCl solution. The crystals are in the form of yellow–green plates. A small plate, cut from a larger crystal, was selected for the X-ray measurements.

$$3(NH_4)_2ReCl_6 + 10C_6H_{13}N + 10HCl + 2H_2O \longrightarrow (C_6H_{14}N)_{10}(ReCl_6)_3{\cdot}4Cl{\cdot}2(H_2O) + 6NH_4Cl$$

Scheme 1. Synthesis of $(C_6\ H_{14}\ N)_{10}\ (ReCl_6)_3{\cdot}4Cl{\cdot}2(H_2O)$.

Yield: 90%.

Elemental analysis calculated (%) for $C_{60}\ H_{144}\ N_{10}\ O_2\ Cl_{22}\ Re_3$ C 30.32 H 6.10, N 5.89, Cl 32.82; found: C 30.26, H 6.05, N 5.32 Cl 32.33. Elemental analysis was conducted using a Vario EL Cube CHNS elemental analyzer from Elementar (Langenselbold, Germany). Samples (2.5–6 mg) were pre-dried in a desiccator prior to measurement.

IR (Nujol MIR, KBr FIR, cm^{-1}): 3429 s νasNH, 2977 m νNH, 2953 m νNH 2524 m νCH, 1704 vs, 1640 m δH_2O, 1589 m δCH, 1549 m δNH_3, 1506 m δNH, 1464 m νCN, 1415 m, 1275 s, 1202 m νCC, 1150 m νCH, 1129 m, 1093 m, 917 m δNH, 855 m νCN, 798 m, 752 m, 695 w δ(ring), 457 m δCNC, 316 vs νRe-Cl, 226 w νRe-Cl, 179 s δCl-Re-Cl, 129 s, δCl-Re-Cl, 150 w δCl-Re-Cl.

2.2. Spectroscopy

IR spectra of the synthesized compounds were recorded using a Bruker VERTEX 70 FTIR spectrometer (Bruker Optics GmbH & Co KG, Germany).

Cary UV-VIS Varian spectrometer was used to obtain electron reflection spectra of powdered samples.

2.3. X-Ray Diffraction Studies and Details of the Structure Refinement

2.3.1. X-Ray Diffraction Experiment

Diffraction data were collected on a Rigaku Oxford Diffraction XtaLAB Synergy-R DW diffractometer (Rigaku Europe SE, Neu-Isenburg, Germany) equipped with a HyPix ARC 150° Hybrid Photon Counting (HPC) detector (Rigaku Europe SE) using CuKα (λ = 1.5418 Å) at 100 K. Data collection, cell refinement, data reduction and analysis were carried out with the CRYSALIS^{PRO} ver. 1.171.43 (Rigaku Oxford Diffraction Ltd., Abignon, UK, 2020). An analytical absorption correction was applied with the use of CRYSALIS^{PRO} RED [13].

CCDC number of compounds **1 2574490** contains the supplementary crystallographic data for this paper. These data are provided free of charge by The Cambridge

Crystallographic Data Center via www.ccdc.cam.ac.uk/data_request/cif (accessed on 15 November 2026).

Selected X-ray data are shown in Tables S1–S5.

2.3.2. Crystal Structure Refinement

The crystal structure was solved with Intrinsic Phasing using the SHELXT program and refined using SHELXL (2015 release) [14,15] with anisotropic thermal parameters for non-H atoms. In the final refinement cycles, water H atoms were located on difference Fourier maps and treated with DFIX restraints to set O-H bond lengths at 0.85 Å. Other H atoms were placed in their calculated positions and refined with a riding model. A disordered chlorido ligand in an Re2-containing anion was modeled in two components with half occupancies (Cl9a and Cl9b). Several C atoms in an N5-containing cation were found to be disordered and refined with 0.5 occupancy factors.

2.3.3. Powder Diffractometry

The powder X-ray diffraction patterns for powdered samples were recorded at RT using a PANanalytical Aeries Instrument Suite X-ray diffractometer with Ni-filtered $CuK_{\alpha 1+2}$ radiation ($K_{\alpha 1+2}$, $\lambda = 1.5418$ Å). The step rate was 0.0109° within the range of 5.003–90.003° 2θ. For simulation of a powder diffractogram, Mercury software was used [16].

2.4. Studies of the Magnetic Properties

Magnetic susceptibility data were collected using a Quantum Design MPMS-XL5 SQUID magnetometer over the temperature range of 300–1.9 K. Magnetic data were corrected for diamagnetic contributions, which were estimated from Pascal's constants, and for temperature-independent paramagnetism.

The diamagnetic contribution of the involved atoms was corrected using Pascal's constants [17].

3. Results and Discussion

The reported multicomponent crystals consist of protonated cyclohexylammonium cations, hexachloridorhenate(IV) anions, chloride anions and water molecules (Tables 1 and 2). Basic crystallographic data, bond lengths and angles, as well as atomic coordinates, are included in the Supplementary Materials [Tables S1–S5]. This compound crystallizes in the triclinic crystal system with space group type $P\overline{1}$.

The symmetry-independent part of the unit cell is presented in Figure 1a.

For the hexachloridorhenate(IV) anions, the Re-Cl bond lengths are listed in Table 2 and fall in the range reported for other hexachloridorhenate(IV) anions from structures reported in the CCDC database [CCDC 1556332 and 1556333]. The Re1-centered $[ReCl6]^{2-}$ anion is essentially octahedral, with Re-Cl distances of 2.3537(4)–2.3704(4) Å and Cl-Re-Cl angles close to the ideal values of 90 and 180°.

Hydrogen bonds of N–H···O, N–H···Cl, O–H···Cl and C–H···Cl could be distinguished (Table 1) with weak-to-medium strength character based on D···A distances. Stronger hydrogen bonds adding to stabilization of the crystal structure are O(1W)–H(1W)···Cl(12) with D···A at 3.1698(16)Å and chloride Cl12 anion as acceptor, as well as N(3)–H(31N)···Cl(12) with D···A at 3.1660(18) Å [18].

Table 1. Analysis of potential hydrogen bonds.

	D–H	H··A	D··A	D–H···A
O(1W)–H(1W)···Cl(12)	0.85(2)	2.39(2)	3.1698(16)	153(2)
O(1W)–H(2W) ···Cl(8) [i]	0.85(3)	2.48(3)	3.3246(16)	169(2)
N(1)–H(11N)···Cl(5) [i]	0.82(3)	2.81(3)	3.4963(18)	143(2)
N(1)–H(12N)···Cl(11) [i]	0.90(3)	2.38(3)	3.2399(19)	161(2)
N(1)–H(13N)···Cl(9a) [ii]	0.90(3)	2.76(3)	3.598(3)	156(2)
N(1)–H(13N)···Cl(9b) [ii]	0.90(3)	2.33(3)	3.191(3)	159(2)
N(1)–H(11N)···Cl(7) [ii]	0.82(3)	2.70(2)	3.372(2)	140(2)
N(2)–H(21N)···O(1W) [iii]	0.92(2)	1.93(2)	2.835(2)	169(2)
N(2)–H(22N)···Cl(2)	0.88(3)	2.79(2)	3.480(2)	138(2)
N(2)–H(22N)···Cl(3) [ii]	0.88(3)	2.76(3)	3.5309(19)	149(2)
N(2)–H(23N)···Cl(11)	0.84(2)	2.42(2)	3.255(2)	172(2)
N(3)–H(31N)···Cl(12)	0.89(3)	2.29(3)	3.1660(18)	170(2)
N(3)–H(32N)···Cl(1) [iv]	0.86(2)	2.62(2)	3.4587(18)	168(2)
N(3)–H(33N)···Cl(12) [iv]	0.88(3)	2.39(2)	3.2522(17)	170(2)
N(4)–H(41N)···Cl(11)	0.85(2)	2.36(2)	3.2066(19)	172(2)
N(4)–H(42N)···Cl(1)	0.89(2)	2.68(2)	3.4759(19)	149(2)
N(4)–H(42N)···Cl(3) [i]	0.89(2)	2.77(2)	3.4487(18)	133.9(19)
N(4)–H(43N)···Cl(12)	0.85(2)	2.37(2)	3.1947(19)	163(2)
N(5)–H(51N)···Cl(11)	0.82(2)	2.38(2)	3.194(2)	172(2)
N(5)–H(52N)···Cl(7)	0.84(3)	2.49(3)	3.279(2)	159(2)
N(5)–H(53N)···Cl(4) [i]	0.97(3)	2.23(3)	3.175(2)	164(3)
C(10)–H(10)···Cl(4) [iv]	1.00(2)	2.81(2)	3.5698(19)	133(3)
C(10)–H(10)···Cl(5) [iv]	1.00(2)	2.64(3)	3.5500(19)	152(3)
C(55)–H(55C)···Cl(2)	0.99(2)	2.82(3)	3.683(2)	146(3)

Symmetry codes: [i] 1−x, 2−y, 1−z, [ii] 1 + x, y, z, [iii] −1 + x, y, z, [iv] 1 − x, 1 − y, 2 − z.

Table 2. Bond lengths and angles in ordered $ReCl_6^{2-}$ anion [Å, °].

Re(1)–Cl(2)	2.3537(4)	Cl(2)–Re(1)–Cl(2) [i]	180.0	Cl(3)–Re(1)–Cl(1)	89.621(15)
Re(1)–Cl(2) [i]	2.3537(4)	Cl(2)–Re(1)–Cl(3) [i]	89.662(15)	Cl(1) [i]–Re(1)–Cl(1)	180.0
Re(1)–Cl(3) [i]	2.3629(4)	Cl(2) [i]–Re(1)–Cl(3) [i]	90.339(15)		
Re(1)–Cl(3)	2.3629(4)	Cl(2)–Re(1)–Cl(3)	90.339(15)		
Re(1)–Cl(1) [i]	2.3704(4)	Cl(2) [i]–Re(1)–Cl(3)	89.660(15)		
Re(1)–Cl(1)	2.3704(4)	Cl(3) [i]–Re(1)–Cl(3)	180.0		
Re(2)–Cl(9A)	2.350(2)	Cl(2)–Re(1)–Cl(1) [i]	89.813(15)		
Re(2)–Cl(6)	2.3510(5)	Cl(2) [i]–Re(1)–Cl(1) [i]	90.187(15)		
Re(2)–Cl(8)	2.3555(5)	Cl(3) [i]–Re(1)–Cl(1) [i]	89.622(15)		
Re(2)–Cl(5)	2.3579(4)	Cl(3)–Re(1)–Cl(1) [i]	90.379(15)		
Re(2)–Cl(4)	2.3625(4)	Cl(2)–Re(1)–Cl(1)	90.188(15)		
Re(2)–Cl(9B)	2.371(2)	Cl(2) [i]–Re(1)–Cl(1)	89.812(15)		
Re(2)–Cl(7)	2.3842(5)	Cl(3) [i]–Re(1)–Cl(1)	90.378(15)		

Symmetry codes ([i]) −x, −y + 1, −z + 2.

Chloride anions Cl11 and Cl12 are involved in the O-H···Cl and N-H···Cl hydrogen bonds with water molecules and ammonium cations as donors, respectively (Table 1).

The O-H···Cl and N-H···Cl interactions show H···Cl distances in the range of 2.23(3)–2.81(3) Å and show D···A distances of 3.1660(18)–3.598(3) Å. Among them, the shortest D···A are observed for O(1W)-H(1W)···Cl(12) [O···Cl = 3.1698(16) Å, H···Cl = 2.39(2) Å, 153(2)°] and N(3)-H(31N)···Cl(12) [N···Cl = 3.1660(18) Å, H···Cl = 2.29(3) Å, 170(2)°], indicating that Cl(12) acts as an important hydrogen bond acceptor. Likewise, Cl(11) is involved in several N-H···Cl interactions, including N(4)-H(41N)···Cl(11) and N(5)-H(51N)···Cl(11), with N···Cl distances of 3.2066(19) and 3.194(2) Å and bond angles of 172(2)°. The water molecule O(1W) is involved in the hydrogen bonding network both as a donor to chloride

ions and as an acceptor in the N(2)-H(21N)···O(1W) contact [N···O = 2.835(2) Å, 169(2)°], thereby linking the ammonium cations and chloride anions into an extended 3D hydrogen-bonded framework.

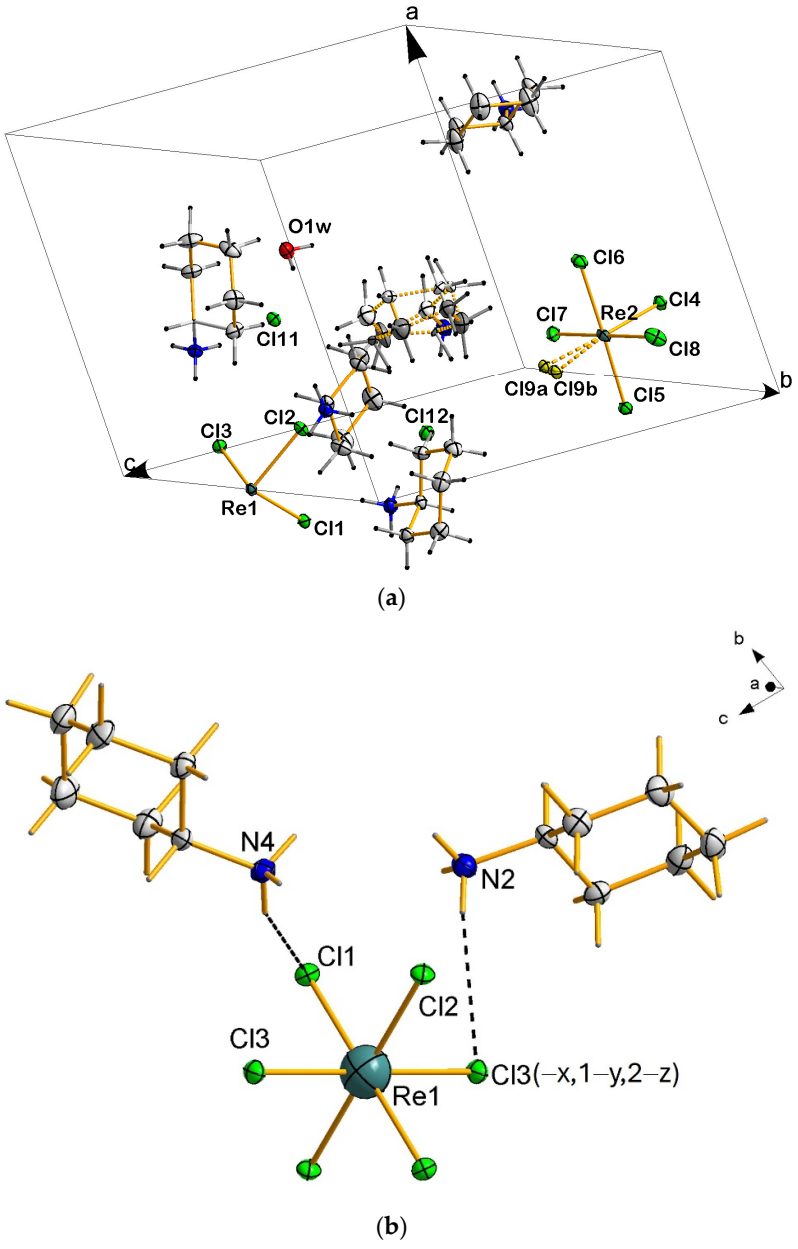


Figure 1. (**a**) Asymmetric unit of $(C_6H_{14}N)_{10}(ReCl_6)_3{\cdot}4Cl{\cdot}2(H_2O)$. Bond lengths of the disordered part are drawn with dashed lines. Thermal ellipsoids are drawn at 50% probability. (**b**) $[ReCl_6]^{2-}$ anion interacting via hydrogen bonds with cyclohexylammonium cations. Thermal displacement ellipsoids are plotted at 50% probability levels.

$[ReCl_6]^{2-}$ anions in the crystal structure are linked to cyclohexylammonium cations via N-H···Cl hydrogen bonds [19,20]. The corresponding structural motif is shown in Figures 1b and 2. Characteristic $R^4_4(12)$ graph-set motifs could be distinguished [21].

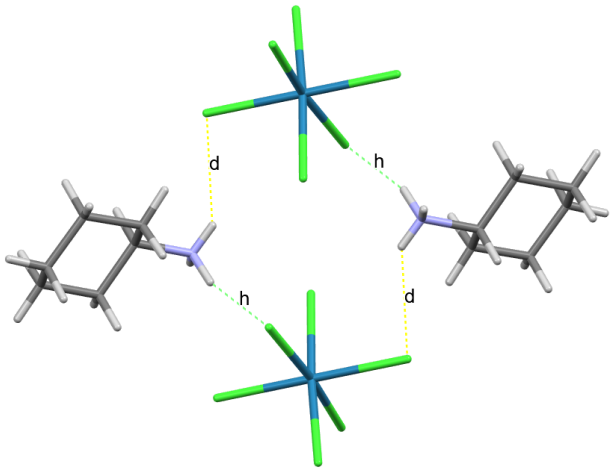
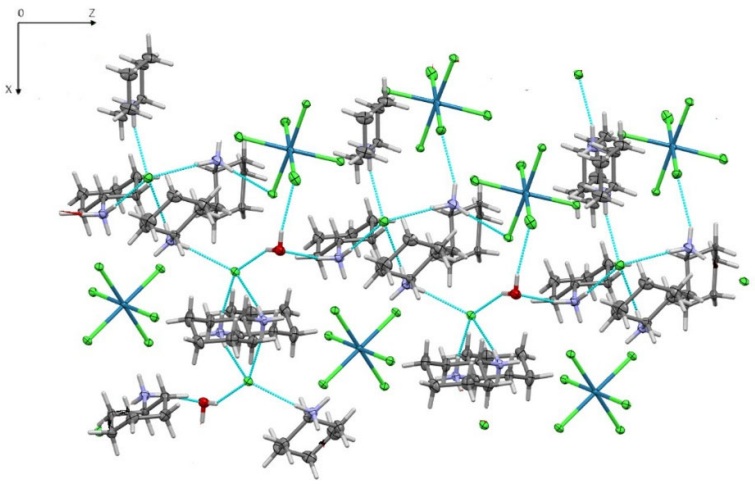
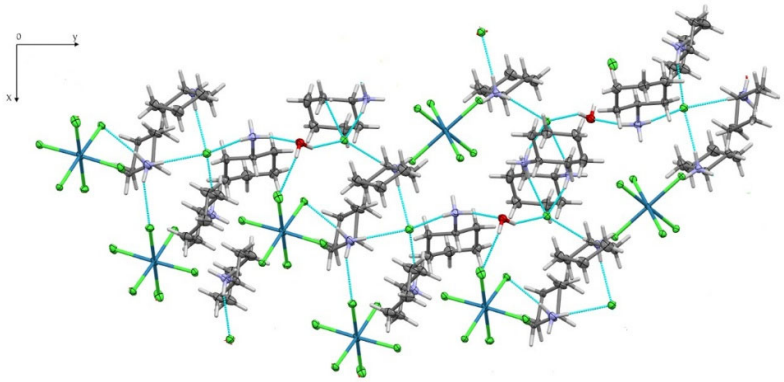


Figure 2. Graph-set motif of $R^4_4(12)$ > d < h > d < h; type present in the crystal structure. Stick model is used for clarity; disordered part is omitted.

These motifs form layers alternating with cyclohexylammonium-containing layers, as shown in Figure 3.



(**a**)



(**b**)

Figure 3. (**a**,**b**) Layered arrangement in the crystal structure. Disordered part is omitted for clarity (only one component is shown). Thermal ellipsoids are drawn at 50% probability. Hydrogen bonds are marked with dashed lines.

Magnetic properties of salts containing $[ReX_6]^{2-}$ anions have been described in the literature [19,20]. However, significantly less information is available for multicomponent crystals. In most cases, antiferromagnetic interactions between paramagnetic Re(IV) centers are postulated, although several factors affect the resulting magnetic behaviors, including zero-field splitting of the $S = 3/2$ ground state. The strength of these interactions depends on the type of halogenide ligand and the halogenide···halogenide distances. The strongest interactions have been reported for iodidorhenate(IV) complexes [22]. Synthesis and characterization of the ionic salts of rhenium(IV) of formula $(Cat)_2[ReI_6]$ with a variety of inorganic and organic cations have been reported. The magnetic properties of these salts were investigated in the temperature range 2–300 K. The reported tetraphenylarsonium salt behaves as a magnetically diluted Re(IV) complex with a large value for the zero-field splitting of the ground level ($|2D| = 49.8\ cm^{-1}$). In contrast, other reported salts, including the sodium salt, were found to be typically antiferromagnetically coupled systems with susceptibility maxima at low temperatures in the order of 20 K. Such magnetic interactions could also be assisted by hydrogen bonds.

Reference [23] reports magnetic susceptibility data, combined with neutron diffraction data [24] for $K_2[ReCl_6]$ and $K_2[ReBr_6]$ and shows presence of antiferromagnetic interactions below 12 and 14 K, respectively, which could point to a canted case (especially if Neel temperature cannot be determined). On the other hand, bulky cations such as NBu_4^+ or $AsPh_4^+$ could lead to magnetic dilution and weakening of X···X interactions. Figgis, Lewis and Mabbs reported on magnetic susceptibilities of simple mononuclear Re^{IV} salts: K_2ReCl_6, Cs_2ReCl_6 and K_2ReF_6 [25].

In this study, the bulky cyclohexylammonium cations prevent strong X···X interactions, whereas the extensive hydrogen bonding network could play a more significant role in transmission of magnetic interactions. The mean Re···Re distances are of 6.67(5) Å which could promote antiparallel arrangements of Re(IV) spins (Figure 4a,b show possible spin arrangements).

Normally for mononuclear hexachloridorhenate(IV) systems ground state is assumed as $^4A_{2g}$ with three unpaired electrons and the first excited state is assumed as $^4T_{2g}$ which stems from the free ion ground state ^4F. Splitting of the $^4T_{2g}$ state is connected with splitting of the ground state in zero field via Equation (1) [26].

$$D = 4\lambda^2\left(\frac{1}{\Delta_{II}} - \frac{1}{\Delta_{\perp}}\right) \quad (1)$$

This behavior can be interpreted as spin state $S = 3/2$ subjected to spin Hamiltonian (Equation (2)) below:

$$H = D\left[S_Z^2 - 1/3\ S(S\ +\ 1)\right]\ +\ g_{II}\beta H_Z S_Z + g_{\perp}\beta\left(H_x S_x + H_y S_y\right) \quad (2)$$

where the first part corresponds to zero-field splitting and the two remaining parts represent the Zeeman effect.

For interpretation of magnetic data, the following equation was selected, describing the temperature dependence of the octahedral tetravalent ion with the zero-field splitting D and J parameters [27,28]. This model is suitable for description of octahedral complexes of d^3 transition metals and allows for determination of the basic parameters described below [29,30].

$$\chi_{II} = \frac{N\beta^2 g^2{}_{II}}{4kT}\ \frac{1 + 9\exp\left(-\frac{2D}{kT}\right)}{1 + exp\left(-\frac{2D}{kT}\right)exp\left(\frac{J}{kT}\right)}$$

$$\chi_{\perp} = \frac{N\beta^2 g^2{}_{\perp}}{4kT}\left\{1 + exp\left(-\frac{2D}{kT}\right)\right\} + 3N\beta^2 g^2{}_{\perp}\frac{tanh\left(\frac{D}{kT}\right)}{4D}\cdot\left\{\left(\frac{kT}{J}\right)tan\ h\left(\frac{J}{2kT}\right) + \left[sec\ h^2\left(\frac{J}{2kT}\right)\right]/2\right\}$$

where D corresponds to ZFS, N is Avogadro number, g is Lande factor, β is Bohr magneton, k is the Boltzmann constant, and T is absolute temperature. As magnetic susceptibility data were collected for a powdered sample, mean values were considered.

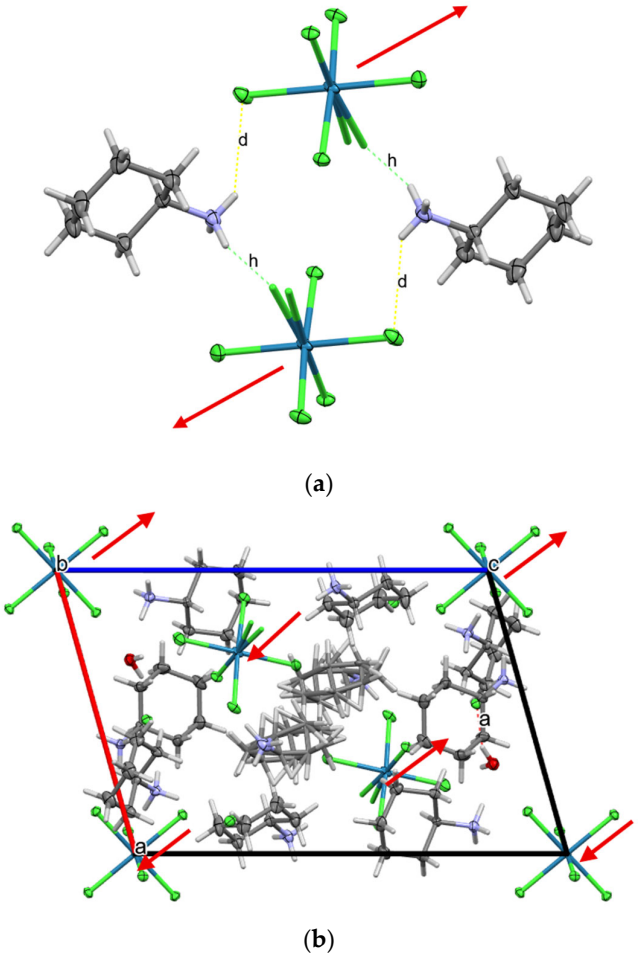


Figure 4. (**a**,**b**) Suggested Re(IV) spin arrangements in the crystal structure. The disordered part is omitted for clarity.

Magnetic susceptibility data were normalized taking 2376.34 g/mol as molar mass. TIP (temperature-independent magnetism) contribution was included as $3630(20) \times 10^{-6}$ cm^3 mol^{-1}. Diamagnetic corrections were applied with Pascal's constants (see Materials and Methods). Least-squares fits were performed using Microsoft Excel software.

The bulk structure has been confirmed with analytical methods (elemental analysis, IR spectroscopy) and powder diffractometry (see the Supplementary Materials).

The simultaneous analysis led to the following best-fit parameters: $D = 6.3$ cm^{-1}, $g_{\parallel} = 1.749$ and $g_{\perp} = 1.810$, and $J = -7.14$ cm^{-1} with $F = 1.93 \times 10^{-5}$ (F is the agreement factor defined as $\Sigma[P_{exp} - P_{calcd}]^2/\Sigma[P_{exp}]^2$ where P is the physical property under study). In this approach the reliability of D value might be limited; at the same time, D and J are correlated.

The magnetic properties of a compound in the form of a plot of $\chi_M T$ against T (χ_M is the magnetic susceptibility per one Re^{IV} ion) are shown in Figure 5. At room temperature, $\chi_M T$ is equal to 1.302 cm^3 mol^{-1} K, a value which is of foreseeable magnitude for a magnetically isolated rhenium(IV) ion, although some lowering is observed due to the presence of antiferromagnetic Re...Re interactions (the expected $\chi_M T$ value is ca. about from 1.59 to 1.87 cm^3 mol^{-1} K for $S_{Re} = 3/2$ and $g_{Re} = 1.86$). Upon cooling, this value remains constant

until 80 K, and then it decreases to reach 0.035 cm^3 mol^{-1} K at 1.9 K. The observed drop in $\chi_M T$ values over the whole temperature range might be justified in terms of the presence of antiferromagnetic interactions. Figure 6 below shows data collected at different magnetic field values, 0.05, 0.5 and 1 T, respectively.

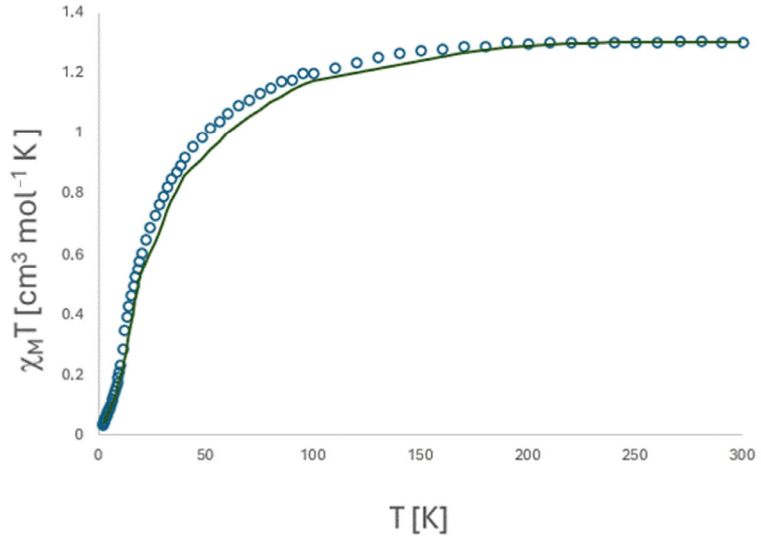


Figure 5. Temperature dependence of $\chi_m T$ (○) of (1). The solid line represents the calculated curve.

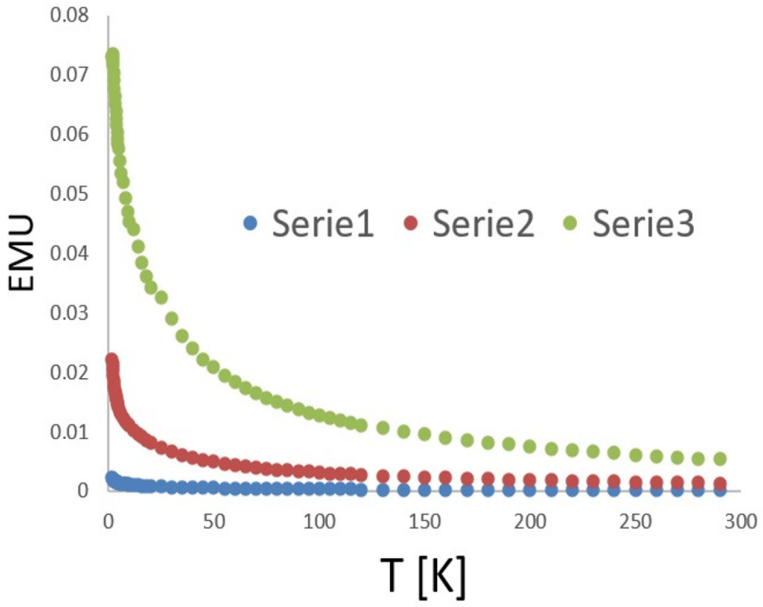


Figure 6. Field-dependent magnetic data—series 1, 2, 3 at 0.05, 0.5 and 1 T, respectively.

Electron spectra

In Re(IV) complexes with d^3 electron configuration, ground state is ^4F. In the octahedral ligand field of the $[ReCl_6]^{2-}$ anion, this state is split, giving rise to the $^4A_{2g}$ ground state. The following spin-allowed electronic transitions are expected:

$$^4A_{2g}(F) \longrightarrow {}^4T_{2g}(F)$$

$$^4A_{2g}(F) \longrightarrow {}^4T_{1g}(F)$$

$$^4A_{2g}(F) \longrightarrow {}^4T_{2g}(P)$$

For Re(IV) compounds, the bands corresponding to $^4A_{2g}(F) \longrightarrow {}^4T_{2g}(F)$ and $^4A_{2g}(F) \longrightarrow {}^4T_{1g}(F)$ transitions are typically observed in the low-energy region of visible light.

The vibronic structure observed between 680 and 780 nm is consistent with coupling of the electronic transitions with Re-Cl vibrational modes (Figure 7). The intense absorption band at approximately 650 nm is consistent with charge-transfer transitions between the Re4+ ion and chloride ligands within the hexachloridorhenate(IV) anion. However, substantial overlap between the CT and d–d absorption bands prevents an unambiguous assignment of the individual transitions.

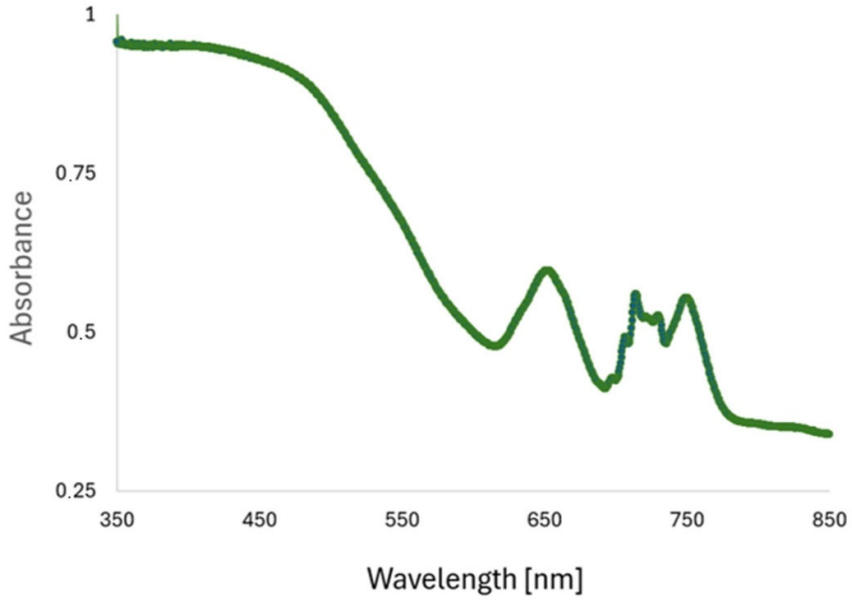


Figure 7. Electron reflection spectra for $(C_6\ H_{14}\ N)_{10}\ (ReCl_6)_3{\cdot}4Cl{\cdot}2(H_2O)$.

4. Conclusions

New multicomponent rhenium(IV) crystals described as $(C_6H_{14}N)_{10}(ReCl_6)_34(Cl){\cdot}2(H_2O)$ were synthesized and characterized by means of single crystal X-ray crystallography, elemental analyses, magnetic susceptibility studies and spectroscopic techniques. These crystals represent an unusual stoichiometry for hexachloridorhenate(IV) anions which are used as dopants in optoelectronic materials and act as model species. Our present study focused on the fundamental properties of the compound, whereas application-relevant demonstration should be pursued in future work. Antiferromagnetic coupling has been detected between the rhenium(IV) centers, with the onset of magnetic ordering at low temperatures and evidence of spin canting. This coupling is likely influenced by a hydrogen bonding network formed with cyclohexylammonium cations. Further investigations, in particular on field-dependent data, are required in the future.

Supplementary Materials: The following supporting information can be downloaded at https://www.mdpi.com/article/10.3390/cryst16110735/s1, Figures S1 and S2, Tables S1–S5. Table S1. Crystal data and structure refinement for $(C_6\ H_{14}\ N)_{10}\ (ReCl_6)_3{\cdot}4(Cl){\cdot}2(H_2\ O)$; Table S2. Atomic coordinates ($\times 10^4$) and equivalent isotropic displacement parameters ($Å^2 \times 10^3$) for $(C_6\ H_{14}\ N)_{10}\ (ReCl_6)_3\ {\cdot}4(Cl){\cdot}2(H_2\ O)$. U(eq) is defined as one third of the trace of the orthogonalized Uij tensor. Table S3. Bond lengths [Å] and angles [°] for $(C_6\ H_{14}\ N)_{10}\ (ReCl_6)_3\ {\cdot}4(Cl){\cdot}2(H_2\ O)$; Table S4. Anisotropic displacement parameters ($Å^2 \times 10^3$) for $(C_6\ H_{14}\ N)_{10}\ (ReCl_6)_3{\cdot}4(Cl){\cdot}2(H_2\ O)$. The anisotropic displacement factor exponent takes the form: $-2\pi^2[\ h^2\ a^{*2}U^{11} + ... + 2\ h\ k\ a^*\ b^*\ U^{12}\ ]$. Table S5. Hydrogen coordinates ($\times 10^4$) and isotropic displacement parameters ($Å^2 \times 10^3$) for $(C_6\ H_{14}\ N)_{10}\ (ReCl_6)_3\ {\cdot}4(Cl){\cdot}2(H_2O)$. Figure S1. Photographies of the investigated crystals. Figure S2. Powder XRD patterns of the investigated compound.

Author Contributions: Conceptualization, A.K.; methodology, A.K.; formal analysis, A.K., N.M., M.H. and Z.F.; investigation, A.K.; resources, A.K.; data curation, A.K.; writing—original draft preparation, A.K., N.M., M.H. and Z.F.; writing—review and editing, A.K., N.M., M.H. and Z.F.; visualization, A.K.; supervision, M.H.; synthesis, A.K., N.M. All authors have read and agreed to the published version of the manuscript.

Funding: This research received no external funding.

Data Availability Statement: Data are available from A.K. Crystal structure and deposited in the CCDC database.

Acknowledgments: The views expressed herein can in no way be taken to reflect the official opinion of the European Space Agency (ESA) and are not intended to endorse particular technologies, companies, or products.

Conflicts of Interest: The authors declare no conflicts of interest.

References

1. Su, Z.; Zhang, B.; Wang, Y.; He, G.; Li, G.; Lin, N.; Yang, K.; He, J.; Liu, S. Broadband rhenium disulfide optical modulator for solid-state lasers. *Photonics Res.* **2018**, *6*, 498–505. [CrossRef]
2. Mahmoud, M.F.; Norazida, A.; Haroon, R.; Nurfarhana, M.S.; Abdulwahhab, E.H.; Mohd Saiful Dzulkefly, Z.; Norazreen, A.A.; Norhana, A. A Review on Rhenium Disulfide: Synthesis Approaches, Optical Properties, and Applications in Pulsed Lasers. *Nanomaterials* **2021**, *11*, 2367. [CrossRef]
3. Saeedi, A.M.; Timoumi, A.; Moussa, Z.; Altass, H.M.; Albetran, H.M.; Ahmed, S.A. Unique physico-chemical characteristics of TiO_2 containing rhenium for advanced energy storage and optoelectronic devices. *Results Surf. Interfaces* **2026**, *22*, 100696. [CrossRef]
4. Cotton, F.A.; Daniels, L.M.; Schmulbach, C.D. Treatment of the octachlorodirhenate ion with high-pressure carbon monoxide; preparation and structure of [*cis*-$Re(CH_3CN)_4(CO)_2]_2$ [$ReCl_6$]. *Inorg. Chim. Acta* **1983**, *75*, 163–167. [CrossRef]
5. Lis, T.; Starynowicz, P. The structure of α,α′-dithiobisformamidinium chloride pentachloro(thiourea)rhenate(IV) (I) and bis(α,α′-dithiobisformamidinium) dichloride hexachlororhenate(IV) trihydrate (II). *Acta Crystallogr. C* **1985**, *41*, 1299–1302. [CrossRef]
6. Piccinelli, F.; Bettinelli, M.; Cano, J.; Lloret, F.; Julve, M.; Dolmella, A. Magnetic Properties of a New Hexahalorhenate(IV) Compound and Structural Comparison with Its Hexahaloplatinate(IV) Analog. *Eur. J. Inorg. Chem.* **2020**, *2020*, 2246–2252. [CrossRef]
7. Armentano, D.; Barquero, M.A.; Rojas-Dotti, C.; Moliner, N.; De Munno, G.; Brechin, E.K.; Martínez-Lillo, J. Enhancement of Intermolecular Magnetic Exchange through Halogen···Halogen Interactions in Bisadeninium Rhenium(IV) Salts. *Cryst. Growth Des.* **2017**, *17*, 5342–5348. [CrossRef]
8. Mroziński, J.; Kochel, A.; Lis, T. Crystal structure and magnetic properties of hexachlororhenates(IV) with aromatic amine cations. *J. Mol. Struct.* **2002**, *641*, 109–117. [CrossRef]
9. Gong, D.-P.; Chen, J.-F.; Zhao, Y.; Cao, D.-K. Bisthienylethene Th_2im and its complex $(Th_2imH)_2[ReCl_6]$: Crystalline-phase photochromism, and photochemical regulation of luminescence and magnetic properties. *Dalton Trans.* **2016**, *45*, 3443–3449. [CrossRef]
10. Armentano, D.; Martinez-Lillo, J. Anion-Assisted Crystallization of a Novel Type of Rhenium(IV)-Based Salt. *Cryst. Growth Des.* **2016**, *16*, 1812–1816. [CrossRef]
11. Li, B.; Huang, Z.; Cai, P.; Zhan, Y.; Feng, X.; Pu, X.; Bi, S.; Wang, G.; Zhang, J.; Liu, Z. Enhanced VIS-NIR emission of Re^{4+} doped Cs_2ZrCl_6 for optical thermometry and near-infrared illumination applications. *Inorg. Chem. Front.* **2024**, *11*, 5157–5171. [CrossRef]
12. Watt, G.W.; Thompson, R.J. Potassium Hexachlororhenate (IV) and Potassium Hexabromorhenate (IV). *Inorg. Synth.* **1963**, *7*, 190–191.
13. Rigaku Oxford Diffraction Ltd. *Computer Programs: CrysAlis PRO, Rigaku OD, 2015*; Rigaku Oxford Diffraction Ltd.: Abingdon, UK, 2020.
14. Sheldrick, G.M. Crystal structure refinement with SHELXL. *Acta Cryst.* **2015**, *C71*, 3–8. [CrossRef]
15. Sheldrick, G.M. A Short History of SHELX. *Acta Cryst.* **2008**, *A64*, 112–122. [CrossRef]
16. Macrae, C.F.; Sovago, I.; Cottrell, S.J.; Galek, P.T.A.; McCabe, P.; Pidcock, E.; Platings, M.; Shields, G.P.; Stevens, J.S.; Towler, M.; et al. Mercury 4.0: From visualization to analysis, design and prediction. *Appl. Cryst.* **2020**, *53*, 226–235. [CrossRef]
17. Bain, G.A.; Berry, J.F. Diamagnetic Corrections and Pascal's Constants. *J. Chem. Educ.* **2008**, *85*, 532–536. [CrossRef]
18. Desiraju, G.R.; Steiner, T. *The Weak Hydrogen Bond in Structural Chemistry and Biology*; Oxford University Press: New York, NY, USA, 1999.
19. Fan, P.; Wanga, L.; Zhang, H. Pyridine-4-carboximidamidate chloride. *Acta Cryst.* **2009**, *E65*, o2408. [CrossRef]

20. Willett, R.D.; Gómez-García, C.J.; Twamley, B.; Gómez-Coca, S.; Ruiz, E. Exchange Coupling Mediated by N–H···Cl Hydrogen Bonds: Experimental and Theoretical Study of the Frustrated Magnetic System in Bis(o-phenylenediamine)nickel(II) Chloride. *Inorg. Chem.* **2012**, *51*, 5487–5493. [CrossRef]
21. Iwama, S.; Takahashi, H.; Tsue, H.; Tamura, R. Case Study on the Interpretation of Crystal Structures Inducing Preferential Enrichment Based on the Graph Set Analysis of Hydrogen Bond Motifs. *Cryst. Growth Des.* **2015**, *15*, 3052–3062. [CrossRef]
22. González, R.; Chiozzone, R.; Kremer, C.; De Munno, G.; Nicolò, F.; Lloret, F.; Julve, M.; Faus, J. Magnetic studies on hexaiodorhenate(IV) salts of univalent cations. Spin canting and magnetic ordering in $K_2[ReI_6]$ with $T_c = 24$. *Inorg. Chem.* **2003**, *42*, 2512–2518. [CrossRef]
23. Martínez-Lillo, J.; Cano, J.; Wernsdorfer, W.; Brechin, E.K. The Effect of Crystal Packing and Re^{IV} Ions on the Magnetisation Relaxation of $[Mn_6]$-Based Molecular Magnets. *Chemistry* **2015**, *21*, 8790–8798. [CrossRef]
24. Rojas-Dotti, C.; Sanchis-Perucho, A.; Orts-Arroyo, M.; Moliner, N.; González, R.; Lloret, F.; Martínez-Lillo, J. Field-Induced Single-Ion Magnet Phenomenon in Hexabromo- and Hexaiodorhenate(IV) Complexes. *Magnetochemistry* **2020**, *6*, 20. [CrossRef]
25. Figgis, B.N.; Lewis, J.; Mabbs, F.E. The magnetic properties of some d^3-complexes. *J. Chem. Soc.* **1961**, *164*, 3138–3145. [CrossRef]
26. Busey, R.H.; Sonder, E. Magnetic Susceptibility of Potassium Hexachlororhenate (IV) and Potassium Hexabromorhenate (IV) from 5° to 300°K. *J. Chem. Phys.* **1962**, *36*, 93–97. [CrossRef]
27. Bertin, A.; Dey, T.; Breuning, D.; Gorkov, D.; Jenni, K.; Krause, A.; Becker, P.; Bohat'y, L.; Khomskii, D.; Pomjakushin, V.; et al. Interplay of magnetic order and ferroelasticity in the spin-orbit coupled antiferromagnet K_2ReCl_6. *Phys. Rev. B* **2024**, *109*, 094409. [CrossRef]
28. Figgis, B.N. Magnetic properties of transition metal ions in asymmetric ligand fields. Part 1.—Cubic field *A* and *E* terms. *Trans. Faraday Soc.* **1960**, *56*, 1553–1558. [CrossRef]
29. Reynolds, P.A.; Delfs, C.D.; Figgis, B.N.; Henderson, M.J.; Moubaraki, B.; Murray, K.S. Magnetic exchange and zero-field splitting in the $d^3[Os^VCl_6]^-$ ion. *J. Chem. Soc. Dalton Trans.* **1992**, *21*, 2309–2312. [CrossRef]
30. Kahn, O. *Molecular Magnetism*; Wiley–VCH: New York, NY, USA, 1993. [CrossRef]

Disclaimer/Publisher's Note: The statements, opinions and data contained in all publications are solely those of the individual author(s) and contributor(s) and not of MDPI and/or the editor(s). MDPI and/or the editor(s) disclaim responsibility for any injury to people or property resulting from any ideas, methods, instructions or products referred to in the content.